

Alma Mater Studiorum Università di Bologna
Archivio istituzionale della ricerca

Detection of trends in magnitude and frequency of flood peaks across Europe

This is the final peer-reviewed author's accepted manuscript (postprint) of the following publication:

Published Version:

Mangini, W., Viglione, A., Hall, J., Hundecha, Y., Ceola, S., Montanari, A., et al. (2018). Detection of trends in magnitude and frequency of flood peaks across Europe. *HYDROLOGICAL SCIENCES JOURNAL*, 63(4), 493-512 [10.1080/02626667.2018.1444766].

Availability:

This version is available at: <https://hdl.handle.net/11585/634657> since: 2019-04-04

Published:

DOI: <http://doi.org/10.1080/02626667.2018.1444766>

Terms of use:

Some rights reserved. The terms and conditions for the reuse of this version of the manuscript are specified in the publishing policy. For all terms of use and more information see the publisher's website.

This item was downloaded from IRIS Università di Bologna (<https://cris.unibo.it/>).
When citing, please refer to the published version.

(Article begins on next page)

This is an Accepted Manuscript of an article published by Taylor & Francis in Hydrological Sciences Journal on 14 March 2018, available online:
<http://www.tandfonline.com/10.1080/02626667.2018.1444766>

Without prejudice to other rights expressly allowed by the copyright holders, this publication can be read, saved and printed for research, teaching and private study. Any other noncommercial and commercial uses are forbidden without the written permission of the copyright holders.

Detection of trends in magnitude and frequency of flood peaks across Europe

Walter Mangini ^a, Alberto Viglione ^a, Julia Hall ^a,
Yeshewatesfa Hundecha ^b, Serena Ceola ^c, Alberto Montanari ^c,
Magdalena Rogger ^a, Jose Luis Salinas ^a, Iolanda Borzi ^d, Juraj Parajka ^{a*}

^a *Institute of Hydraulic Engineering and Water Resources Management, Vienna University of Technology, Karlsplatz 13 E222/2, 1040, Vienna, Austria.*

^b *Swedish Meteorological and Hydrological Institute, Folkborgsvägen 17, 601 76, Norrköping, Sweden.*

^c *Department of Civil, Chemical, Environmental and Material Engineering, University of Bologna, Viale Risorgimento 2, 40136, Bologna, Italy.*

^d *Department of Engineering, University of Messina, Piazza Salvatore Pugliatti 1, 98122, Messina, Italy.*

*Corresponding author: Juraj Parajka,

Tel: +43-1-58801-22311, e-mail address: parajka@hydro.tuwien.ac.at,

Postal address: J. Parajka at TU Wien E222/2, Karlsplatz 13, 1040, Vienna, Austria

18

19 **Detection of trends in magnitude and frequency of flood peaks across**
20 **Europe**

21 This study analyses the differences in significant trends in magnitude and frequency of
22 floods obtained from Annual Maximum Flood (AMF) and Peak Over Threshold (POT)
23 flood peak series. Flood peaks are identified from European daily discharge data for the
24 period 1965-2005, using a baseflow-based algorithm and significant trends in AMF
25 series are compared with POT series, derived for six different exceedance thresholds.
26 Results show that more trends in flood magnitude are detected in the AMF than the
27 POT series and for the POT series more significant trends are detected in flood
28 frequency than in flood magnitude. Spatial coherent patterns of significant trends are
29 detected, which is further investigated by stratifying the results into five regions based
30 of catchment and hydro-climatic characteristics. All data and tools used in this study are
31 open-access and results are fully reproducible.

32

33 Keywords: Annual Maximum Flood, Europe, flood frequency, flood magnitude,
34 Peak Over Threshold, trend.

35 Highlights: Consistent regional patterns of significant trends in flood magnitude
36 and flood frequency are detected across Europe using freely available daily
37 discharge time series. Flood trends are sensitive to the method used to define the
38 flood peak series. The paper supports the value of open data and tools for the
39 advance of hydrological science, ensuring the full reproducibility of the
40 analyses.

1. Introduction

Recently, numerous extreme flood events have been recorded across the European continent, such as the central European floods in summer 2002 and 2013 (Ulbrich et al. 2003, Blöschl et al. 2013, Schröter et al., 2015), floods in England in summer 2007 and winter 2013 (Marsh 2008, Muchan et al. 2015) and flash flooding in western Italy in autumn 2011 (Marchi et al., 2013). As many of these and other recent flood events are perceived unprecedented, there is a growing concern that flooding in Europe has become more frequent and severe.

Accounting for possible changes in floods is important for hydrological applications, such as design of flood protection facilities, risk assessment and risk management (Parry et al. 2007, Kundzewicz 2012, Rosner et al. 2014). Additionally, accounting for temporal trends in flood peak series may lead to better flood frequency estimates (Khaliq et al. 2006, Renard et al. 2006, Vogel et al. 2011, Šraj et al. 2016).

To detect changes in floods, several analyses have been performed for different regions in Europe. Examples of recent studies include but are not limited to: Hannaford and Buys (2012) for Great Britain, Murphy et al. (2013) for Ireland, Giuntoli et al. (2012) in France, Arheimer and Lindström (2015) in Sweden, Blöschl et al. (2011) and Jeneiova et al. (2016) in Austria, Brázdil et al. (2006, 2012), Kundzewicz et al. (2013) and Pekárová et al. (2016) in the Central Europe, and Bard et al. (2012) for the Alpine mountain range region. Such analyses provided insight into regional patterns of flood changes within selected catchment, national or regional boundaries. Hall et al. (2014) performed a meta-analysis of published literature on flood change across Europe. They found large-scale patterns of flood changes with similar sign of change but also concluded that the studies are not fully comparable, due to different time periods

analysed and differences in the methodology applied to derive flood series and to detect flood changes.

When performing trend tests on flood series, the main methodological concerns include the definition of the variable “flood”. Commonly two different methods are used to derive times series of flood peaks, the Annual Maximum Flood (AMF) series and the Peak Over Threshold Flood (POT) series. The AMF series consists of the largest discharge values per each year, with the main advantage that the events selected in two successive years are generally considered independent. However, the AMF approach does only consider a small number of flood peaks and does not take into account the flood events that are lower than the annual maximum, but may be relevant to society, particularly in terms of damages.

The POT series (also denoted as Partial Duration Series), consists of flood peaks exceeding a predefined threshold (Cunnane 1973, Madsen et al. 1997). If the POT series is used, it is important to ensure that the peaks are independent (e.g. do not occur on the recession curves of the preceding flood peak). The advantage of the POT compared to the AMF series is that it allows not only the detection of trends in the mean magnitude of flood peaks exceeding a threshold (trends in magnitude) but also trends in the mean number of flood events per year (trends in frequency).

Large-scale studies using the POT flood series with high spatial resolution do not exist in Europe so far. An example of a continental scale study can be found in Hirsch and Archfield (2015) and Archfield et al. (2016) for the US. The authors found no consistent national wide trend in the flood series signal but some regional trend pattern. In Europe, there are examples of studies aiming to characterise changes in floods adopting the POT approach, but those analyses use either high spatial resolution databases at a regional scale (Petrow and Merz 2009, Vormoor et al. 2016) or

continental database with only a small number of stations (Mediero et al. 2015). In all these studies, the threshold values for the selection of the POT series have been chosen by fixing a mean number of events per year or per season (in general 1, 2 or 3 events) but, to our knowledge, no systematic analysis to detect the effect of the threshold selection on the trend detection results together with their spatial patterns was performed so far. Méndez et al. (2006) underlines that: “The selection of the threshold implies a balance between bias and variance. Too low a threshold will likely violate the basis of the model, causing bias; too high a threshold will identify few extremes, leading to high variance”.

The main objective of this paper is therefore to detect trends across Europe, derived from AMF and POT flood peaks series. The following research questions are being addressed:

- (1) What are the patterns of trends in both flood magnitude and frequency across Europe for the period 1965-2005?
- (2) What is the sensitivity of the detected trends to the selection criterion used to define different flood peak series?
- (3) What are the larger scale morpho-climatological characteristics of the catchments with significant trends?

The analysis is performed on a large open-source dataset comprising 629 gauging stations with daily mean discharges. All data and tools used here are open-access and available at the SWITCH-ON portal (<http://www.water-switch-on.eu>).

2. Methodology

Changes in flood magnitude and frequency are detected by performing trend analysis on flood peak series. The flood peak series are compiled using a procedure based on (i) separating independent discharge events employing a baseflow separation algorithm, (ii) selecting the maximum daily discharge within each individual event as the peak event and (iii) sampling those events to be considered flood peaks, according to the different AMF or POT approaches. The first two parts of the methodology are described in section 2.1, the selection of flood peaks is elaborated in section 2.2 and the methodologies used for trend detection are presented in section 2.3.

2.1 Identification of independent peak events

Trend tests are based on the assumption that data are identically distributed and independent (WMO 2009). Two consecutive extreme events can be assumed physically independent when they are caused by different forces, so that the previous event does not condition the occurrence of the second event.

While the AMF approach leads to flood events that are generally considered independent, an objective selection criterion is needed within the POT approach for obtaining independent flood peaks. Generally, the independence criteria are related to the concept of streamflow recession, which states that the independence of two flood events increases over time if the discharge between them is decreasing.

Therefore, one possible criterion for defining temporal independence of the peaks within the POT series is to define a minimum number of days between two successive events, either by using a predefined value, e.g. 15 days (Mallakpour and Villarini 2015) or by determining a time lag as direct function of the catchment size

(Svensson et al. 2005). Another possible independence criterion that has been suggested by the USWRC (1982), is the introduction of an additional condition concerning the intermediate discharge magnitude between two successive peaks, as for example applied in Mediero et al. 2015.

In the present work, the criterion of independence is fulfilled using a baseflow-based algorithm. The algorithm allows the separation of independent discharge peak events by comparing the recorded total flow and the estimated baseflow. The maximum daily mean discharge within each separated event can then be considered an independent discharge peak event.

The traditional procedure for the baseflow estimation starts with identification of the points at which the direct runoff component of a hydrograph (i.e. surface runoff) starts and, successively, ends. The start and end points are normally identified as the point in time when the flow starts to increase, or a plot of logarithmic transformed discharge values against time becomes a straight line, respectively.

In this study, the Chapman digital filter (Chapman 1999) was applied. The digital filter estimates the baseflow as a simple weighted average of the direct runoff and the baseflow at the previous time interval:

$$Q_b(i) = k \cdot Q_b(i-1) + (1-k) \cdot Q_d(i) \quad (1)$$

where $Q_b(i-1)$ and $Q_d(i)$ are the baseflow at time interval $i-1$ and the direct runoff at time interval i , respectively, and the parameter k is the recession constant during periods of no direct runoff. Assuming that the recorded total flow $Q(i)$ is the sum of baseflow $Q_b(i)$ and direct runoff $Q_d(i)$, then the $Q_b(i)$ can be estimated as:

$$Q_b(i) = \frac{k}{1-k} \cdot Q_b(i-1) + \frac{1}{1-k} \cdot Q_d(i) \quad (2)$$

The estimation of the recession constant k for each catchment follows the approach suggested in Vogel and Kroll (1996) and successive applications (Thomas et al. 2013). The approach consists of the following steps:

- (1) Identification of the start/end of the discharge recession, defined as the point in time when a 3-day centred moving average begins to decrease/increase;
- (2) Rejection of the recessions shorter than 10 days;
- (3) Removal of the first three points of the recession to eliminate the effect of the moving average;
- (4) For each recession identified, a regression $\ln(Q) = \ln(Q_0) + \ln(k_i) \cdot t + \text{residual}$ is fitted, applying the ordinary-least-squares method;
- (5) Computing the average of the estimated regression slope k_i , for individual events, to approximate the recession constant k .

Once the recession constant k is estimated, the baseflow Q_b is calculated using the Chapman filter. The direct runoff Q_d is obtained as the difference between the recorded total flow and the estimated baseflow. Discharge events are defined here as independent if they are separated by intervals within which the direct runoff is lower than the baseflow or lower than the mean annual direct runoff (to remove the instances when discharge or baseflow equals zero). The maximum discharge value within each discharge event is then selected as independent flood peak.

Fig. 1 shows a sample application of the baseflow-based algorithm for the peak separation in the river Teme at Tembury, Western England (catchment area 1134 km²) for the year 1968. The figure shows the total discharge time series, the estimated baseflow, the start and end points of the identified discharge event and the independent flood peaks for each separated event.

2.2 Selection of flood series

Flood series are compiled from the discharge peaks identified by the methodology in Section 2.1 using two different approaches: the Annual Maximum Flood (AMF) and the Peak Over Threshold (POT) selection approach.

AMF are commonly identified by a so-called “block maximum” approach (Gumbel, 1958). This method requires the time series to be divided into blocks of equal length and the largest value within each block to be selected. The main advantage of this method is that the immediate correspondence with the “Return Period” concept can be made, considering one year as time unit. One limitation of the method is that annual peaks with very small values may be included (e.g. in drier years), whereas in years with several larger floods only the largest value is considered.

The POT method identifies all flood events that exceed a given threshold. Unlike the AMF approach, the POT methodology allows the analysis of both trends in magnitude (POT-M) and trends in frequency (POT-F).

When performing trend analysis on flood series using the POT approach, the number of floods to be included in the series is determined by selecting an appropriate threshold. Many studies use a fixed mean number of exceedances per year (λ) to identify the appropriate threshold value. In the specific case of this study, the length of the time series analysed is 41 years: if λ is chosen to be one (POT1), the highest 41 discharge peaks are considered to form the flood series. By formulating the hypothesis that flood events follow a Poisson process, λ represents the event rate (or frequency) per unit time of the distribution.

In this paper, the sensitivity of the trend results to the selection of the threshold is assessed for a mean number of exceedances per year λ ranging from one to six (POT1 to POT6). Additionally, trends in the flood magnitude series of POT1 are compared to those of AMF.

To be able to better interpret trends results for flood magnitude obtained for different flood series, the Multiple Index (MI) is defined here as:

$$MI = Q_F / Q_A \quad (3)$$

where Q_F is the mean discharge value of a flood peak series and Q_A is the mean annual discharge recorded for an individual station. Thus, MI indicates how large are the flood peaks in different AMF and POT flood series compared to annual mean flow at each individual station. The MI also indicates for which λ , the POT flood time series represents only larger or combination of larger and smaller flood events.

2.3 Trend analysis and test for statistical significance

Trend detection can be performed using parametric or non-parametric approaches. Parametric tests, such as a simple linear regression over time, are useful for the easy representation and interpretation of the trend results (Merz et al. 2012), but need an a-priori assumption on the regression function and require specific statistical characteristics such as normal distribution of the residuals and constant variance (Helsel and Hirsch 2002). If those conditions are not satisfied, non-parametric procedures, such as Mann-Kendall test (Kendall 1938) are preferred. In the present analysis, the Mann-Kendall rank correlation test is adopted for the detection of monotonic trends in flood magnitude and the Theil-Sen-slope algorithm (Sen 1968) is used for a non-parametric trend slope estimation.

For the analysis of trends in flood frequency in the POT series, the Chi-squared test of significance on the parametric Poisson regression is used. The Mann-Kendall test has not been applied to the POT-F series, as the presence of several paired values (such as series of counts), the rank correlation procedure may fail in finding a hierarchy in the series (Frei and Schär 2001, Vormoor et al. 2016). The Poisson regression is a generalised linear regression model able to fit count series. The model assumes the counts to be Poisson distributed with the logarithm of their expected value varying linearly with time. The Chi-squared significance test assesses whether the slope parameter of the regression differs significantly from zero, which means that a significant trend in flood frequency is detected. Trends presented in this paper are tested with a two-tailed test at a 10% significance level. For these trends, the corresponding one-tailed tests for the same test statistic is to be considered either twice as significant (half the p-value, 5%), if the trend is in the direction specified by the test (e.g., positive), or not significant at all (p-value above 0.05), if the trend is in the direction opposite that specified by the test (e.g., negative).

The presence of autocorrelation within time series is checked here for both the AMF and POT frequency (POT-F) series. In both cases, the Breusch-Godfrey (Breusch 1978) test for the presence of serial correlation in time series is used. The test is performed because serially correlated time series tend to “artificially” show higher significance in the trends when trend tests are used (von Storch 1999). Test for serial correlation of the POT magnitude (POT-M) series was not performed, since that would require advanced interpolation methodologies (Rehfeld et al. 2011), which are out of the scope of the present paper.

3. Data

3.1 A Pan-European peak discharge dataset

The data used in the analysis is based on the 1235 stations listed in the European subset of the Global Runoff Data Centre database (GRDC 2016), recording daily discharge values. The average record length of time series considered is 54 years, the available record length differs considerably between individual stations and possible selected time periods(Fig. 2).

In order to maximise both the spatial and temporal coverage of the discharge time series, a common time window of 41 years (1965-2005) is chosen (Fig. 2). Time series with more than 2 years of missing data in the time window are excluded, in order to minimise inhomogeneities within the data, which resulted in 629 gauging stations to be included in the trend analysis.

As the aim of this study is to compare the large scale spatial patterns of trends detected in different flood peak series, all time series satisfying the above mentioned criteria are included and no distinction is made between the causes of trends (such as climate, river training or dam construction), as this is outside the scope of this study.

3.2 Catchment characteristics

As this study is also interested in determining the relation between large scale morpho-climatological characteristics of the catchments and significant trends in flood series, the following four catchment characteristics are estimated: catchment area, mean catchment elevation, mean annual rainfall and mean annual air temperature evaluated for the period 1965-2005.

For each catchment the mean elevation is calculated from the European Digital Elevation Model provided by the European Environment Agency (EEA 2016a), with a spatial resolution of 1000 m, while the mean annual precipitation and air temperature are derived from the E-OBS gridded dataset (Haylock et al. 2008). Catchment boundaries for each gauging station have been determined from the Catchment Characterisation and Modelling version 2.1 (CCM2) dataset (Vogt et al. 2007). The calculated catchment characteristics and the shape files of the catchment boundaries are openly accessible and included in the Supplementary material of this paper.

3.3 Hydro-climatic regions

In order to stratify the results of flood trend detection across Europe, the stations are grouped into five regions: Alpine, Atlantic, Boreal, Continental and Mediterranean regions. The subdivision is based on the biogeographical regions of Europe singled out by the European Environment Agency (EEA 2016b). The hydro-climatic regions are shown in Fig. 3, along with the selected gauging stations, and their description is given in Table 1. The predominant climate of each region is derived from the digital dataset of the Köppen-Geiger climate classification (Köppen 1884, Kottek et al. 2006).

The Alpine region includes the main mountain ranges in Europe: the Alps, the Scandes, the Pyrenees and the Carpathians. Despite their different geographical position, the Alpine region exhibit a number of common features including altitudinal gradients, climatic influence, soil types, geology and vegetation types. The Alps influence the climate of central Europe and divides the Mediterranean region in the south and the temperate region in the north. The Alps are the origin of the many major European rivers such as the Adige, Danube, Po, Rhone and Rhine. About 70 % of the

Alpine region is influenced by human activities (EEA 2002) and the majority of rivers are affected by production of hydro-electric power. The Alpine region encompasses the largest number stations that are included in the analysis.

The Atlantic region is situated along the Atlantic coast and includes Great Britain, Ireland, the Netherlands, the northern shores of Spain and Portugal, and the coastal parts of Germany, Denmark, Belgium and France. The region mainly consists of small hills or flatland and is influenced by an oceanic temperate climate, resulting in relatively mild winters and summers and high rainfall rates throughout the year (EEA 2002). In the region, several large rivers such as the Gironde, Loire, Rhine, Seine, Schelde and Thames drain into the Atlantic Ocean.

The Boreal region covers Estonia and Latvia, South-eastern Norway and most of Sweden, Finland, the northern parts of Lithuania and Belarus and parts of eastern Russia. It is a transition zone between the Arctic and temperate regions of Europe. The climate can be described as cool-temperate mainly sub-continental, with relatively long periods of snow cover (several months) and relatively short growing season (EEA 2002). Most of the region is situated below 500 m a.s.l. Glacial and post-glacial erosion has formed large and undulating plains.

The Continental region covers large areas between Denmark and Sweden in the north and Italy and Balkan region in the south. The region intersects parts of the Alpine region. The climate is continental with strong contrasts between warm summers and cold winters in the central and eastern parts. Precipitation is mainly received during the summer months. In the north, the landscape is flat and becomes increasingly hilly in the south with large flood plains along the large rivers (e.g. the Danube, Desna, Dnepr, Dnestr, Elbe, Loire, Oder, Pripyat, Rhine, Vistula or Volga) (EEA 2002).

The Mediterranean region is situated between the Atlantic region in the west and the Continental and Alpine regions in the north. The climate is dry and warm, with hot summers and mild winters. Hills and mountains dominate the landscape, with the low mountain ranges being intersected by inland plateaus. In the Mediterranean region, there is a pronounced variability in climate and topographic characteristics due to a variety of small scale landscape characteristics such as slope, exposition, geology and the distance to the sea (EEA 2002). The largest rivers draining into the Mediterranean Sea are the Adige, Drin-Bojana, Ebro, Neretva, , Rhone and Tiber. This region contains the smallest number of gauging stations.

4. Results

4.1 Frequency of discharge peak events

Fig. 4 shows the spatial pattern of the mean number of independent discharge peak events per year, identified according to the procedure presented in the section 2.1. The panels around the map give typical two-year example of the variability of different runoff hydrographs across the five hydro-climatic regions.

Fig. 5 summarises the results of the discharge peaks identification based on the five regions and shows the variability of the mean number of independent peaks per year identified across Europe.

The highest number of peaks is observed in the Atlantic and Alpine region, with a median value of ~ 16 events per year. In the Atlantic region, 10% of stations exhibit a mean number of peaks per year larger than 30, most of which are situated in northern England and Scotland (Fig. 4). A lower median mean number of peaks per year (14) is found in the Continental region the median, as well as the upper 10 percentile (16).

In the Boreal and Mediterranean region, the median mean number of peaks per year is the lowest. In particular, in the Boreal region, snow accumulation and melting processes dominates the runoff regime, resulting in the smallest number of peaks. In this region, not more than a mean of five peaks per year can be identified in many catchments. In the arid Mediterranean region, the variability of the mean number of peaks per year within a region is the lowest (Fig. 5). The median mean number of peaks events in this region is 10 independent events per year.

4.2 Trends in AMF and POT1 series

The results of trend detection in Annual Maximum Flood series (AMF) are presented in Fig. 6. Significant positive and negative trends in AMF series are detected at 61 (10%) and 48 (8%) stations respectively, both at a 5% significance level, whereas the other 520 stations show no evidence of a significant trend. This means that, when considering the whole dataset, the number of detected significant trends are more than what could be expected by chance. Moreover, large-scale spatially coherent patterns of trends with the same direction can be identified. These trend patterns are of practical importance and indicate the possibility of common drivers. Therefore, a description of the trends found in the individual regions is given below. The largest number of stations (23) exhibiting significant positive trends in AMF series is found in the Atlantic region (21 stations in Great Britain and two in the western France), while only six stations (three in England and three smaller catchments in southern France) exhibits significant negative trends in the same region.

A large number of stations exhibiting either significant increasing (16 stations) or decreasing (13 stations) trends in AMF series is detected in the Continental region.

Increasing trends are observed in the eastern France, in the upper Danube and in three large catchments in Central Germany (Lahn, Neckar and Rhine rivers). Decreasing trends are observed in large catchments (Schwarze Elster, Havel and Oder River) in the eastern Germany and few small catchments in southern France.

Significant decreasing trends are mostly detected in the Alpine region (19 stations). These catchments are located in the south-eastern France (near the border with Switzerland) and southward of the main ridge of Central Alps in Austria and Tatra Mountains in Slovakia. Increasing flood trends in Alpine region tend to be detected in small catchments, having mean catchment area of about 200 km². These catchments are located in central Switzerland, Tirol and southern Bavaria.

In the Boreal region, four and seven stations show increasing or decreasing trends, respectively. While increasing flood trends are detected in two catchments in Finland and two catchments in southern Sweden, negative trends are detected in three small catchments (catchment area smaller than 10 km²) located in the southern part of Sweden and four larger catchments in Southern Finland and Eastern Sweden.

In the Mediterranean region, no clear pattern of flood trends can be found: three catchments exhibit increasing flood trends but also three stations with decreasing flood trends are found.

Interestingly, stations exhibiting significant changes in AMF series present a mean number of peaks per year very close to the median mean values of each individual regional distributions. Exceptions are the catchments exhibiting trends in the Atlantic region, in which the mean numbers of peaks per year belong to the upper part of the regional distribution.

The trend analysis on Peak Over Threshold (POT) series is presented next in Fig. 7, which shows the results of setting the threshold λ a mean of 1 events per year (POT1), with respect to trends in flood magnitude (POT1-M, left panel) and trends in flood frequency (POT1-F, right panel).

The left panel of Fig. 7 shows the spatial pattern of flood change detected in the POT1-M series. The total number of stations exhibiting significant trends in POT1-M series is slightly lower than the number of stations exhibiting trends in AMF series. The AMF (exactly one flood event per year) and POT1 (an average of one event per year) series can be compared, given the same sample size and 5% significance level of the one-sided tests. Interestingly, trends in POT1-M series and AMF series are not always detected in the same catchments, which results in a different spatial pattern of flood change in the two cases.

Significant positive or negative trends in POT1-M series are detected in 57 (9%) and 40 (6%) stations, respectively. Similarly to the trends detected in AMF, the number of detected trends are more than what could be expected by chance, when considering the whole dataset. Also in the case of POT1, spatially coherent patterns of trend can be found. The majority of catchments with increasing trends is situated in the Continental (31 stations, mostly in Germany) and Alpine (16 stations, situated mostly in Bavaria and Tirol) region. Only eight catchments in the Atlantic region exhibit increasing trends in POT1-M series, a relatively small number compared to the significant trends detected in AMF series.

Significant negative trends in POT1-M series are detected in 19 catchments in the Boreal region (Scandinavia), which is almost three times more than what is detected in AMF series. Moreover, less negative trends in POT1-M series are detected (10 stations) in the Alpine region (southern Austria, Slovenia) compared to AMF series.

Significant trends in POT1-F series (Fig.7, right panel) are detected in 133 stations. In particular, an increasing trend in POT1-F series is detected in 68 (11%) stations, and a decreasing trend in 65 (10%) stations. This would suggest that the trends in frequency are significant for Europe as a whole. Again, when considering the hydro-climatic regions independently discernible spatial patterns emerge. The highest number of the catchments exhibiting either positive or negative trends in POT1-F series are situated in the Atlantic region (29 stations in Great Britain out of 37 in the region) and in the Alpine region (35 stations, mostly in Central and East Alps, Slovenia and rivers originating in Tatra Mountains in Slovakia), respectively.

4.3 Sensitivity of flood trends to the selection of different flood series

The trends in flood magnitude in the AMF and POT1-M series (Fig. 6 and 7) indicated different spatial patterns of flood changes across Europe. The next section in this paper investigates the sensitivity of trends in POT series with regard to the selection of different exceedance thresholds λ .

Generally, different exceedance thresholds imply an increasing number of flood peaks considered for increasing λ . While POT1-M series represent a compilation of the largest floods recorded at each gauging station, an increase in λ determines a lower threshold and therefore an increase in the number of (smaller) events considered.

Fig. 8 shows the variability of the Multiple Index (MI), the ratio between the mean discharge magnitude of the flood series and the mean annual discharge for individual stations, estimated for the AMF and the different POT-M flood series in the five hydro-climatic regions. The MI of the POT1-M series is the largest, while results

indicate that the MI of the AMF series tends to be slightly bigger than the MI of the POT2-M series in all the regions. The smallest MI is estimated in POT6-M flood series.

The median value of the MI in POT1-M series ranges between four (i.e. 4 times the mean annual flow) in the Boreal region to more than 23 in the Mediterranean region. This result can be explained by the different hydrological flood regimes across Europe. On one side, the arid climate of the Mediterranean region implies a dry mean discharge regime during the year that is offset by intense precipitation events leading to extreme values. Moreover, the subset of stations in the Mediterranean region considered here is mainly composed of small catchments, which have an intrinsically high variance in the hydrograph. On the other side, snowmelt processes drive the extreme values in the Boreal region. In this case, the volume of the peak is large but the maximum intensity reached remains in the order of magnitude of the mean discharge regime.

The sensitivity of trends in POT series to the selection of different exceedance thresholds λ is assessed for a mean number of floods per year ranging from 1 to 6 (i.e. POT1 to POT6). Table 2 and 3 present the absolute number of trends detected in the flood series in each regions.

Similarly, Fig. 9 shows the percentage of stations exhibiting significant positive or negative trends, both tested at 10% significance level, for the six different exceedance thresholds, grouping the stations into the five hydro-climatological regions.

The almost horizontal lines in Figure 9 suggest that results of trend analyses in POT series are not very sensitive to the selection of the threshold, with the exception of trends in flood frequency in the Mediterranean and Boreal region. In particular, with increasing the mean number of events per year λ , a greater amount of significant negative trends in flood frequency are detected in the Western part of the Mediterranean

region (i.e. Southern France), while significant positive trends increase in number in the Boreal catchments situated on the coast.

Top panel of Fig. 9 shows the percentage of significant increasing and decreasing trends in POT1-M to POT6-M series. The percent number of stations exhibiting significant trends and the general regional tendency differs significantly between the regions.

In the Alpine and Boreal regions, decreasing trends dominate, with exception for the POT1-M series in the Alpine region. The largest number of stations exhibiting decreasing trends in the Alpine region is observed in POT6-M series, while the Boreal region exhibits the most relevant negative trends in the floods series containing the highest peaks (POT1-M).

The general tendency in the Atlantic region is the opposite, except for the POT1-M series, significant increasing trends are observed in POT2 to POT6 series at more than 15% of stations.

In the Continental region, the highest percentage of positive trends is detected in POT1-M series while, considering higher λ thresholds, the number of stations exhibiting significant trends is smaller and the general tendency differs. However, from POT1-M to POT4-M series, positive trends dominate. When including smaller floods in POT5-M and POT6-M series, a larger number of stations exhibit decreasing trends is found.

In the Mediterranean region, a prevailing tendency towards increasing flood magnitude is found, but the number of stations included in the region is rather small to be able to draw general conclusions.

Bottom panel of Fig. 9 shows the significant trends detected in POT-F series. A clear tendency towards increasing flood frequency is found in the Atlantic, which is even more evident when considering lower λ values (POT1-F or POT2-F series).

Significant negative trends in flood frequency are detected in the Continental and Alpine region, where decreasing trends are much more apparent in all series when compared to the trends in flood magnitude for the same regions.

Significant positive trends in flood frequency are found in the Boreal region and the percentage of stations exhibiting this tendency increases for increasing λ . From POT3-F to POT6-F series, the increase in flood frequency is observed in more than one station out of three. Interestingly, only a very small number of catchments exhibits concurrent significant trends in both flood frequency and magnitude.

An opposite pattern compared to the Boreal region is found in the Mediterranean region, where a higher percentage of significant decreasing trends are detected for increasing λ .

While significant trends can be regionally considered not very sensitive to the selection of the threshold (apart for the cases analysed above), trends detected at individual stations may considerably change over the different flood series.

Fig. 10 and 11 summarise, for each individual station, the results of trends detected in flood magnitude (comparing AMF and POT-M) series and frequency (considering only POT-F series), respectively. The diverging colour scale indicates the intensity of the decadal change (% per decade) detected in the different flood series. Negative trends are depicted with yellow to red colours and positive trends with light to dark blue colours. Only those stations that exhibit a significant trend (at 10%

significance level) in at least one of the different flood series are presented in the figures.

Considering trends in flood magnitude (Fig. 10), between 33% of the stations (in the Atlantic region) and 45% of the stations (in the Boreal region) exhibit trends in at least two different flood series. An exception is the Continental region, where only 21% of the stations exhibit trends in at least two different flood series. If a stricter criterion is used, around 15% of the stations in total exhibits consistent trends in at least three different flood series.

Results differ when considering trends in flood frequency (Fig. 11). In this case, a much more consistent situation is visible over the different thresholds considered: more than 30% of the stations in almost all the regions in Europe exhibit trends in at least three different flood series.

AMF series exhibit the largest intensity of decadal change in flood magnitude, with median values of 9% or 10% per decade for increasing or decreasing trends, respectively. The median intensity of decadal change in POT1-M series is 5% per decade for increasing trends and 4% per decade for decreasing trends, while lower median intensities are detected in the other POT-M series (POT2-M to POT6-M).

The magnitude of changes in flood frequency is small and decreases significantly with increasing exceedance threshold, with similar values for increasing and decreasing trends. The median intensity of change in POT1-F series is 0.3 event per decade and decreases to less than 0.14 events per decade in POT6-F series.

Interestingly, both for trends in magnitude and frequency, no inversions in sign of significant trends detected with different thresholds are found out.

In order to test the sensitivity of the results to the representativeness of coverage of stations and to the issue of sites with human interventions, all analyses above have been repeated in two cases: (1) by removing randomly all sites with the same river name but one (i.e., removing 22% of the sites); (2) by removing all sites for which a step change in the time series of runoff flashiness, quantified by the ratio of absolute day-to-day fluctuations of streamflow relative to total flow in a year (see Holko et al., 2011), has not been detected by the Pettitt test at the 10% significance level (i.e., removing 41% of the sites). In both cases, essentially the same conclusions have been obtained as those showed here (see Supplementary material Figures S1 and S2 for a comparison with Figure 9).

4.4 Physiographic characteristics of catchments exhibiting significant changes in flood magnitude and frequency

Fig. 12 shows the distribution of the mean elevation (top left panel), area (top right panel), mean annual precipitation (bottom left panel) and mean annual air temperature (bottom right panel) of those catchments which exhibit significant increasing or decreasing trends in flood magnitude. Categories along x-axes indicate the different flood series considered: AMF and POT1-M to POT6-M series.

Results indicate that the significantly increasing trends in flood magnitudes detected in AMF series and POT-M series selected by high mean number of exceedance per year λ (i.e. POT3-M, POT5-M and POT6-M) tend to occur more often in low-elevation watersheds, with mean elevation below 400 m asl. The flood series of the largest floods (POT1-M) have an opposite tendency, which is decreasing flood magnitude in catchments having low mean elevation. However, there is a clear tendency towards increasing flood magnitudes in catchments having a high mean annual air

temperature and high mean annual precipitation rates. Conversely, a relationship between catchment size and significant trends cannot be seen.

Fig. 13 shows a clear pattern of increasing flood frequency in catchments with low mean catchment elevation and low mean annual air temperature, particularly for POT2 and higher λ_s . These catchments are also characterised by a lower mean annual precipitation, when compared to catchments exhibiting decreasing trends in flood frequency. Again, no clear relationship between the size of catchments and the detected trends can be found.

5. Discussion and conclusions

The overall aim of this study is to contribute to the detection of flood trends in Europe. Compared to previous works, three novel aspects have been investigated. First, the comparison of two different methods used to derive flood series at the European scale: the Annual Maximum Flood (AMF) and the Peak Over Threshold (POT) approach. Second, the sensitivity analysis of flood trends with respect to different exceedance thresholds in the POT approach. Third, the full reproducibility of the analyses is given, supporting the value of open data and tools for the advance of hydrological science.

Previous regional or continental studies in Europe have analysed the spatial pattern of flood trends either in predefined regions, as discussed by Kundzewicz (2012) and Hall et al. (2014), or in regions exhibiting similar flood regime based on clustering techniques (Parajka et al. 2010, Mediero et al. 2015). In this study, regional patterns are analysed in predefined regions based on a biogeographical classification of Europe (EEA 2016b). The Alpine, Atlantic, Boreal, Continental and Mediterranean regions used here to stratify the trend results correspond approximately to the three main regions (Atlantic western Europe and northern Europe, Continental central Europe and eastern Europe, and the European Mediterranean) identified in Hall et al. (2014) or with the five regions derived from cluster analysis presented by Mediero et al. (2015) which allows a comparison of the results cross these papers.

When considering Europe as a whole, the percent of stations with statistically significant trends (10% significance level for the two-sided tests, 5% level for the one-sided tests), across all types of flood series, is more than what would be expected by chance alone. Moreover, coherent larger-scale spatial patterns of significant trends can be identified across the European continent for different series of flood peaks. For example, a general tendency towards increasing flood magnitude and frequency is found

in Atlantic region. The flood magnitude increases more in AMF series and POT-M series selected by lower exceedance threshold λ . A significant increase in flood magnitude in flood series with high peaks (i.e. POT1-M, POT2-M) is only detected in few stations, but trends in flood frequency are more apparent when considering the same thresholds (i.e. POT1-F, POT2-F). The increasing trends detected in AMF are consistent with the main findings of Hannaford and Buys (2012) and Murphy et al. (2013) for England and Ireland, respectively, but for slightly different time periods.

In the Boreal region, a clear tendency towards increasing flood frequency and decreasing flood magnitude is detected in POT series. This is in line with the main findings presented in Hall et al. (2014), for the northern part of Eastern Europe and Scandinavia. Differently, no apparent pattern of change in flood magnitude is detected when considering AMF series (Fig. 6). Similar conclusions were also drawn by Arheimer and Lindström (2015) for Swedish catchments, in which the authors detected no widespread evidence of flood trends in 69 AMF series.

The Central region presents the highest percentage of stations (17%) exhibiting significant positive trends in magnitude in the POT1-M series. Similarly, Kundzewicz et al. (2013) found that positive trends can be detected in that region with respect to two metrics (flood severity, related to flood frequency, and flood magnitude) when analysing the main flood events over the time period 1985–2009. However, when lowering the threshold λ , a higher number of decreasing trends in flood magnitude and frequency can be detected, especially on the Elbe River. This is in accordance with the negative trends detected in Brázdil et al. (2006, 2012) within the Czech Republic boundaries.

The Alpine region, including the Alps and other main mountain areas of Europe, exhibits similar pattern of flood changes as described in Blöschl et al. (2011) for the

Austrian parts of the Alps. In the northern part of the main alpine ridge, a general tendency for increasing flood trends is detected, while a clear pattern towards decreasing flood magnitude is detected in the southern part of the Alps, particularly for POT series compiled by high λ values (i.e. considering smaller floods). Similar pattern of decreasing flood magnitude are found here in south-eastern France and in the alpine rivers originating in Tatra Mountains. Pattern of flood trends in the POT3 series indicate similar decreasing tendencies, as shown by Mediero et al. (2015).

The Mediterranean region shows a general tendency towards increasing flood magnitude and decreasing flood frequency, especially in series compiled by lower λ . This is in line with results presented in Giuntoli et al. (2012) in French.

From a methodological point of view, this study shows that the number of catchments exhibiting significant changes within a region is consistent over the different thresholds (Fig. 9), with a few exception (such as trends in flood frequency in the Mediterranean and Boreal regions). The detection of trends in flood magnitude and the frequency from POT series is an alternative to AMF approach and indicates regionally consistent trends over the different thresholds. Fig. 10 and 11 show, however, that the number of catchments exhibiting significant changes for a large range of exceedance threshold (> 3 threshold) is rather small, particularly when analysing trends in flood magnitude. Overall, the results show a larger number of stations exhibiting significant changes in flood frequency than in flood magnitude.

Thus, in Europe, similar to the trend analysis of Archfield et al. (2016) in the US, the picture of flood change obtained is strongly heterogeneous and no general statements of uniform trends across the entire continent can be detected, but regional pattern exist.

The regions with consistent spatial patterns of significant trends across the different flood series identified here show that the trends detected can be considered real and not an artefact of the method used to derive the series. Such areas can serve as prime locations for future studies aiming to attribute the trends not only for individual catchments but rather attributing changes with methods that allow for a regional scale assessment such as the scaling fingerprints (Viglione et al., 2016).

Finally, data, tools and results used in the study are openly accessible. In the supplement material, a table listing the station name, geographical coordinates, selected physiographic attributes and the results of trend detection is provided (data access at: <http://www.water-switch-on.eu/sip-webclient/byod/#!/resource/12069>). Daily runoff time series can be obtained from the Global Runoff Data Centre on request, while the derived catalogue of flood peak events can be accessed under the name of “Pan-European catalogue of flood events” in the Spatial Information Platform of the SWITCH-ON portal (data access at <http://www.water-switch-on.eu/sip-webclient/byod/#!/resource/12056>). Following the recommendation of Ceola et al. (2015), the authors believe that the availability of all data, tools and results will allow further advancing the research concerning flood change, as it will facilitate comparison and extension of the current study. Future studies could for example further investigate the controlling factors of flood trends or attribute the spatial patterns of the detected trends to possible drivers.

666

667 **Acknowledgements**

668 This study was performed within the EU FP7-funded project SWITCH-ON [grant numbers
669 603587, 2014], which explores the potential of Open Data for comparative hydrology and
670 collaborative research, as well as promote Open Science for transparency and reproducibility.

671 All data, scripts and protocols are available in the SWITCH-ON Virtual Water-Science
672 Laboratory at www.water-switch-on.eu for review.

673 The work was supported by the ERC Advanced Grant “FloodChange” [number 291152,
674 2011] and the MSCA-ITN-ETN SYSTEM RISK [numbers 676027, 2015].

675 Finally, the authors acknowledge the E-OBS dataset from the EU-FP6 project
676 ENSEMBLES (<http://ensembles-eu.metoffice.com>), the data providers in the ECA&D project
677 (<http://www.ecad.eu>), the Global Runoff Data Centre, 56068 Koblenz, Germany and the CCM
678 River and Catchment Database © European Commission - JRC, 2007 for the data.

679 The paper was developed using Copernicus data and information funded by the
680 European Union - EU-DEM layers.

681

682 **References**

- 683 Archfield, S.A., Hirsch, R.M., Viglione, A., Blöschl, G., 2016. Fragmented patterns of flood
684 change across the United States. *Geophysical Research Letters* **10**, 232–239.
685 doi:10.1002/2016GL070590.
- 686 Arheimer, B., Lindström, G., 2015. Climate impact on floods: changes in high flows in Sweden
687 in the past and the future (1911-2100). *Hydrology and Earth System Sciences* **19**, 771–784.
688 doi:10.5194/hess-19-771-2015.
- 689 Bard, A., Renard, B., Lang, M., 2012. Floods in the Alpine Areas of Europe, in: Zbigniew W.
690 Kundzewicz (Ed.), Changes in Flood Risk in Europe. *IAHS Press and CRC Press/Balkema*,
691 Wallingford, UK, 375–384.
- 692 Blöschl, G., Nester, T., Komma, J., Parajka, J., Perdigão, R.A.P., 2013. The June 2013 flood in
693 the Upper Danube Basin, and comparisons with the 2002, 1954 and 1899 floods. *Hydrology and*
694 *Earth System Sciences* **17**, 5197–5212. doi:10.5194/hess-17-5197-2013.
- 695 Blöschl, G., Viglione, A., Merz, R., Parajka, J., Salinas, L.J., Schöner, W., 2011. Climate
696 impacts on floods and low flows. *Österreichische Wasser- und Abfallwirtschaft* **63**, 21–30.
697 doi:10.1007/s00506-010-0269-z.
- 698 Brázdil, R., Dobrovolný, P., Kakos, V., Kotyza, O., 2006. Historical and recent floods in the
699 Czech Republic: causes, seasonality, trends, impacts, in: Flood Risk Management: Hazards,
700 Vulnerability and Mitigation Measures. *Springer*, Dordrecht, 247–259.
- 701 Brázdil, R., Reznickova, L., Havlicek, M., Elleder, L., 2012. Floods in the Czech Republic, in:
702 Zbigniew W. Kundzewicz (Ed.), Changes in Flood Risk in Europe. *IAHS Press and CRC*
703 *Press/Balkema*, Wallingford, UK, 191–211.
- 704 Breusch, T.S., 1978. Testing for autocorrelation in dynamic linear models. *Australian Economic*
705 *Papers* **17**, 334–355. doi:10.1111/j.1467-8454.1978.tb00635.x.

Ceola, S., Arheimer, B., Baratti, E., Blöschl, G., Capell, R., Castellarin, A., Freer, J., Han, D.,
 Hrachowitz, M., Hundecha, Y., Hutton, C., Lindström, G., Montanari, A., Nijzink, R., Parajka,
 J., Toth, E., Viglione, A., Wagener, T., 2015. Virtual laboratories: new opportunities for
 collaborative water science. *Hydrology and Earth System Sciences* **19**, 2101–2117.
 doi:10.5194/hess-19-2101-2015.

Chapman, T., 1999. A comparison of algorithms for stream flow recession and baseflow
 separation. *Hydrological Processes* **13**, 701–714. doi:10.1002/(SICI)1099-
 1085(19990415)13:5<701::AID-HYP774>3.0.CO;2-2.

Cunnane, C., 1973. A particular comparison of annual maxima and partial duration series
 methods of flood frequency prediction. *Journal of Hydrology* **18**, 257 – 271. doi:10.1016/0022-
 1694(73)90051-6.

EEA, 2002. Biogeographical regions in Europe [online]. *EEA Report No 1/2002*. Available
 from: http://www.eea.europa.eu/publications/report_2002_0524_154909.

EEA, 2016a. Digital Elevation Model over Europe [online]. Available from:
<http://www.eea.europa.eu/data-and-maps/data/eu-dem>.

EEA, 2016b. Biogeographical regions [online]. Available from: <http://www.eea.europa.eu/data-and-maps/data/biogeographical-regions-europe-3#tab-gis-data>.

Frei, C., Schär, C., 2001. Detection Probability of Trends in Rare Events: Theory and
 Application to Heavy Precipitation in the Alpine Region. *Journal of Climate* **14**, 1568–1584.
 doi:10.1175/1520-0442(2001)014<1568:DPOTIR>2.0.CO;2.

Giuntoli, I., Renard, B., Lang, M., 2012. Floods in France, in: Zbigniew W. Kundzewicz (Ed.),
 Changes in Flood Risk in Europe. *IAHS Press and CRC Press/Balkema*, Wallingford, UK, 212–
 224.

GRDC, 2016. The Global Runoff Data Centre [online]. Available from:
http://www.bafg.de/GRDC/EN/Home/homepage_node.html.

731 Gumbel, E.J., 1958. Statistics of extremes, ISBN 0-486-43604-7. ed. *Columbia University*
732 *Press*, New York.

733 Hall, J., Arheimer, B., Borga, M., Brázdil, R., Claps, P., Kiss, A., Kjeldsen, T.R.,
734 Kriaucianienė, J., Kundzewicz, Z.W., Lang, M., Llasat, M.C., Macdonald, N., McIntyre, N.,
735 Mediero, L., Merz, B., Merz, R., Molnar, P., Montanari, A., Neuhold, C., Parajka, J., Perdigão,
736 R.A.P., Plavcová, L., Rogger, M., Salinas, J.L., Sauquet, E., Schär, C., Szolgay, J., Viglione, A.,
737 Blöschl, G., 2014. Understanding flood regime changes in Europe: a state-of-the-art assessment.
738 *Hydrology and Earth System Sciences* **18**, 2735–2772. doi:10.5194/hess-18-2735-2014.

739 Hannaford, J., Buys, G., 2012. Trends in seasonal river flow regimes in the UK. *Journal of*
740 *Hydrology* **475**, 158 – 174. doi:10.1016/j.jhydrol.2012.09.044.

741 Haylock, M.R., Hofstra, N., Klein Tank, A.M.G., Klok, E.J., Jones, P.D., New, M., 2008. A
742 European daily high-resolution gridded data set of surface temperature and precipitation for
743 1950–2006. *Journal of Geophysical Research: Atmospheres* **113**, D20119.
744 doi:10.1029/2008JD010201.

745 Helsel, D.R., Hirsch, R.M., 2002. Statistical Methods in Water Resources Techniques of Water
746 Resources Investigations. *U.S. Geological Survey*.

747 Hirsch, R.M., Archfield, S.A., 2015. Flood trends: Not higher but more often. *Nature climate*
748 *change* **5**, 198–199. doi:10.1038/nclimate2551.

749 Jeneiová, K., Kohnová, S., Hall, J., Parajka, J. (2016) Variability of seasonal floods in the
750 Upper Danube River basin, *J. Hydrol. Hydromech.*, Vol. 64, No. 4, 2016, p. 357 – 366 , doi:
751 10.1515/johh-2016-0037.

752 Kendall, M.G., 1938. A New Measure of Rank Correlation. *Biometrika* **30**, 81–93.

753 Khaliq, M.N., Ouara, T.B.M.J., Ondo, J.-C., Gachon, P., Bobée, B., 2006. Frequency analysis
754 of a sequence of dependent and/or non-stationary hydro-meteorological observations: A review.
755 *Journal of Hydrology* **329**, 534–552. doi:10.1016/j.jhydrol.2006.03.004.

Köppen, W., 1884. Die Waermezonen der Erde, nach der Dauer der heissen, gemaessigten und kalten Zeit und nach der Wirkung der Waerme auf die organische Welt betrachtet (The thermal zones of the Earth according to the duration of hot, moderate and cold periods and to the impact of heat on the organic world). *Meteorologische Zeitschrift* **1**, 215–226. doi:10.1127/0941-2948/2011/105.

Kottek, M., Grieser, J., Beck, C., Rudolf, B., Rubel, F., 2006. World Map of the Köppen-Geiger climate classification updated. *Meteorologische Zeitschrift* **15**, 259–263. doi:10.1127/0941-2948/2006/0130.

Kundzewicz, Z., 2012. Changes in flood risk in Europe. *IAHS Press Wallingford*.

Kundzewicz, Z.W., Pińskwar, I., Brakenridge, G.R., 2013. Large floods in Europe, 1985–2009. *Hydrological Sciences Journal* **58**, 1–7. doi:10.1080/02626667.2012.745082.

Lang, M., Ouarda, T.B.M.J., Bobée, B., 1999. Towards operational guidelines for over-threshold modeling. *Journal of Hydrology* **225**, 103–117. doi:S0022-169499001675.

Madsen, H., Rasmussen, P.F., Rosbjerg, D., 1997. Comparison of annual maximum series and partial duration series methods for modeling extreme hydrologic events: 1. At-site modeling. *Water Resources Research* **33**, 747–757. doi:10.1029/96WR03848.

Mallakpour, I., Villarini, G., 2015. The changing nature of flooding across the central United States. *Nature Climate Change* **5**, 250–254. doi:10.1038/nclimate2516.

Marchi, L., Boni, G., Cavalli, M., Comiti, F., Crema, S., Lucia, A., Marra, F., Zocatelli, D., 2013. The flash flood of October 2011 in the Magra River basin (Italy): rainstorm characterisation and flood response analysis. *Geophysical Research Abstracts* **15**, EGU2013-11125.

Marsh, T., 2008. A hydrological overview of the summer 2007 floods in England and Wales. *Weather* **63**, 274–279. doi:10.1002/wea.305.

780 Mediero, L., Kjeldsen, T.R., Macdonald, N., Kohnova, S., Merz, B., Vorogushyn, S., Wilson,
 781 D., Albuquerque, T., Blöschl, G., Bogdanowicz, E., Castellarin, A., Hall, J., Kobold, M.,
 782 Kriauciuniene, J., Lang, M., Madsen, H., Gül, G.O., Perdigão, R.A.P., Roald, L.A., Salinas,
 783 J.L., Toumazis, A.D., Veijalainen, N., Þórarinnsson, Ó., 2015. Identification of coherent flood
 784 regions across Europe by using the longest streamflow records. *Journal of Hydrology* **528**, 341
 785 – 360. doi:10.1016/j.jhydrol.2015.06.016.

786 Méndez, F.J., Menéndez, M., Luceño, A., Losada, I.J., 2006. Estimation of the long-term
 787 variability of extreme significant wave height using a time-dependent Peak Over Threshold
 788 (POT) model. *Journal of Geophysical Research: Oceans* **111**. doi:10.1029/2005JC003344.

789 Merz, B., Kundzewicz, Z.W., Delgado, J., Hundecha, Y., Kreibich, H., 2012. Detection and
 790 Attribution of Changes in, in: Zbigniew W. Kundzewicz (Ed.), Changes in Flood Risk in
 791 Europe. *IAHS Press and CRC Press/Balkema*, Wallingford, UK, 446–469.

792 Muchan, K., Lewis, M., Hannaford, J., Parry, S., 2015. The winter storms of 2013/2014 in the
 793 UK: hydrological responses and impacts. *Weather* **70**, 55–61. doi:10.1002/wea.2469.

794 Murphy, C., Harrigan, S., Hall, J., Wilby, R.L., 2013. Climate-driven trends in mean and high
 795 flows from a network of reference stations in Ireland. *Hydrological Sciences Journal* **58**, 755–
 796 772. doi:10.1080/02626667.2013.782407.

797 Parajka, J., Kohnová, S., Bálint, G., Barbuc, M., Borga, M., Claps, P., Cheval, S., Dumitrescu,
 798 A., Gaume, E., Hlavčová, K., Merz, R., Pfaundler, M., Stancalie, G., Szolgay, J., Blöschl, G.,
 799 2010. Seasonal characteristics of flood regimes across the Alpine–Carpathian range. *Journal of*
 800 *Hydrology* **394**, 78–89. doi:10.1016/j.jhydrol.2010.05.015.

801 Parry, M.L., Canziani, O.F., Palutikof, J.P., van der Linden, P.J., Hanson, C.E., 2007. IPCC,
 802 2007. Climate change 2007: impacts, adaptation and vulnerability. *Contribution of working*
 803 *group II to the fourth assessment report of the intergovernmental panel on climate change*.

804 Pekárová, P., Pramuk, B., Halmová, D., Miklánek, P., Prohaska, S., Pekár, J., 2016.
805 Identification of long-term high-flow regime changes in selected stations along the Danube
806 River. *Journal of Hydrology and Hydromechanics* **64**, 393–403.

807 Petrow, T., Merz, B., 2009. Trends in flood magnitude, frequency and seasonality in Germany
808 in the period 1951–2002. *Journal of Hydrology* **371**, 129–141.
809 doi:10.1016/j.jhydrol.2009.03.024.

810 Rehfeld, K., Marwan, N., Heitzig, J., Kurths, J., 2011. Comparison of correlation analysis
811 techniques for irregularly sampled time series. *Nonlinear Processes in Geophysics* **18**, 389–404.
812 doi:10.5194/npg-18-389-2011.

813 Renard, B., Lang, M., Bois, P., 2006. Statistical analysis of extreme events in a non-stationary
814 context via a Bayesian framework: case study with peak-over-threshold data. *Stochastic*
815 *Environmental Research and Risk Assessment* **21**, 97–112. doi:10.1007/s00477-006-0047-4.

816 Rosner, A., Vogel, R.M., Kirshen, P.H., 2014. A risk-based approach to flood management
817 decisions in a nonstationary world. *Water Resources Research* **50**, 1928–1942.
818 doi:10.1002/2013WR014561.

819 Schröter, K., Kunz, M., Elmer, F., Mühr, B., Merz, B., 2015. What made the June 2013 flood in
820 Germany an exceptional event? A hydro-meteorological evaluation. *Hydrology and Earth*
821 *System Sciences* **19**, 309–327. doi:10.5194/hess-19-309-2015.

822 Sen, P.K., 1968. Estimates of the Regression Coefficient Based on Kendall's Tau. *Journal of the*
823 *American Statistical Association* **63**, 1379–1389. doi:10.2307/2285891.

824 Šraj, M., Viglione, A., Parajka, J., Blöschl, G., 2016. The influence of non-stationarity in
825 extreme hydrological events on flood. *Journal of Hydrology and Hydromechanics* **64**(4), 426–
826 437. doi:10.1515/johh-2016-0032.

827 Svensson, C., Kundzewicz, W.Z., Maurer, T., 2005. Trend detection in river flow series: 2.
828 Flood and low-flow index series. *Hydrological Sciences Journal* **50**, 811–824.
829 doi:10.1623/hysj.2005.50.5.811.

830 Thomas, B.F., Vogel, R.M., Kroll, C.N., Famiglietti, J.S., 2013. Estimation of the base flow
831 recession constant under human interference. *Water Resources Research* **49**, 7366–7379.
832 doi:10.1002/wrcr.20532.

833 Ulbrich, U., Brücher, T., Fink, A.H., Leckebusch, G.C., Krüger, A., Pinto, J.G., 2003. The
834 central European floods of August 2002: Part 1 – Rainfall periods and flood development.
835 *Weather* **58**, 371–377. doi:10.1256/wea.61.03A.

836 USWRC, 1982. Guidelines for determining flood flow frequency, Bulletin #17B. ed.
837 Interagency Advisory Committee on Water Data. water.usgs.gov/osw/bulletin17b/dl_flow.pdf.

838 Viglione, A., Merz, B., Viet Dung, N., Parajka, J., Nester, T., & Blöschl, G. (2016). Attribution
839 of regional flood changes based on scaling fingerprints. *Water Resources Research*, **52**(7),
840 5322-5340, doi:10.1002/2016WR019036.

841 Vogel, R.M., Kroll, C.N., 1996. Estimation of baseflow recession constants. *Water Resources*
842 *Management* **10**, 303–320.

843 Vogel, R.M., Yaindl, C., Walter, M., 2011. Nonstationarity: Flood magnification and recurrence
844 reduction factors in the United States. *Journal of the American Water Resources Association* **47**,
845 464–474. doi:10.1111/j.1752-1688.2011.00541.x.

846 Vogt, J., Soille, P., De Jager, A., Rimaviciute, E., Mehl, W., Foisneau, S., Bodis, K., Dusart, J.,
847 Paracchini, M.L., Haastруп, P., Bamps, C., 2007. A pan-European River and Catchment
848 Database. *OPOCE*. doi:10.2788/35907.

849 Von Storch, H., 1999. Measures of Statistical Analysis in Climate Research. Analysis of Climate
850 Variability: *Applications of Statistical Techniques Proceedings of an Autumn School Organized*

851 *by the Commission of the European Community on Elba from October 30 to November 6, 1993,*
852 11–26. doi:10.1007/978-3-662-03744-7_2.

853 Vormoor, K., Lawrence, D., Schlichting, L., Wilson, D., Wong, W.K., 2016. Evidence for
854 changes in the magnitude and frequency of observed rainfall vs. snowmelt driven floods in
855 Norway. *Journal of Hydrology* **538**, 33–48. doi:10.1016/j.jhydrol.2016.03.066.

856 WMO, 2009. Extreme value analysis, in: WMO Commission for Hydrology (Ed.), Management
857 of Water Resources and Application of Hydrological Practices, 1–59.

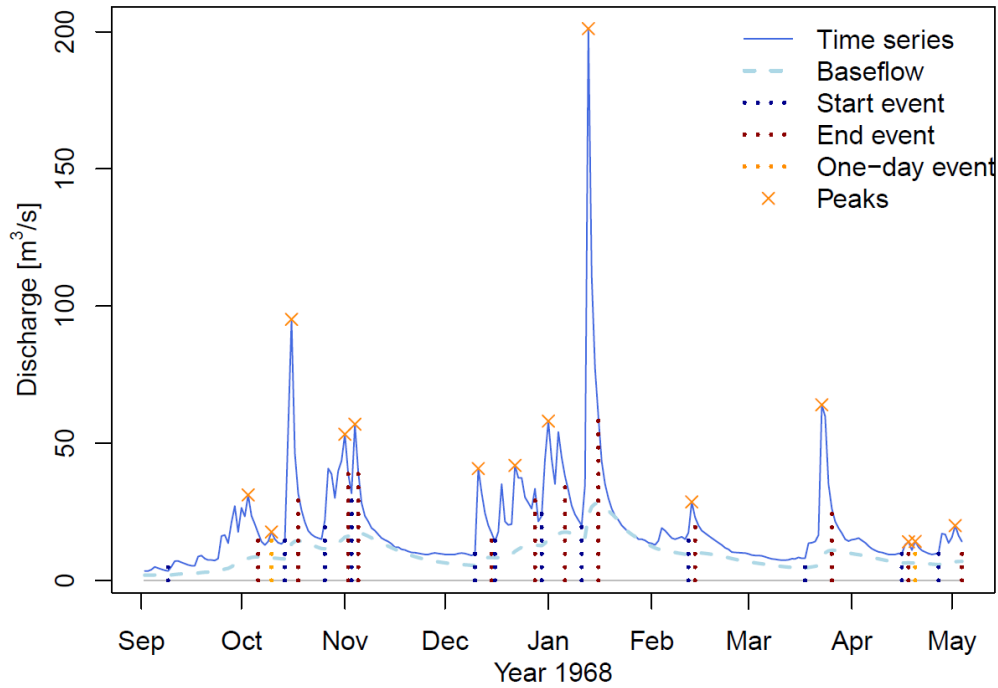


Figure 1. Example of discharge events and peak flows (crosses) for river Teme, at Tenbury station (UK). A discharge event starts (vertical dashed dark blue line) when the direct runoff is larger than the baseflow (light blue dashed line), and ends (vertical dashed red line) when it is lower. One-day long events are shown with vertical dashed orange lines, independent peak discharges as orange crosses.

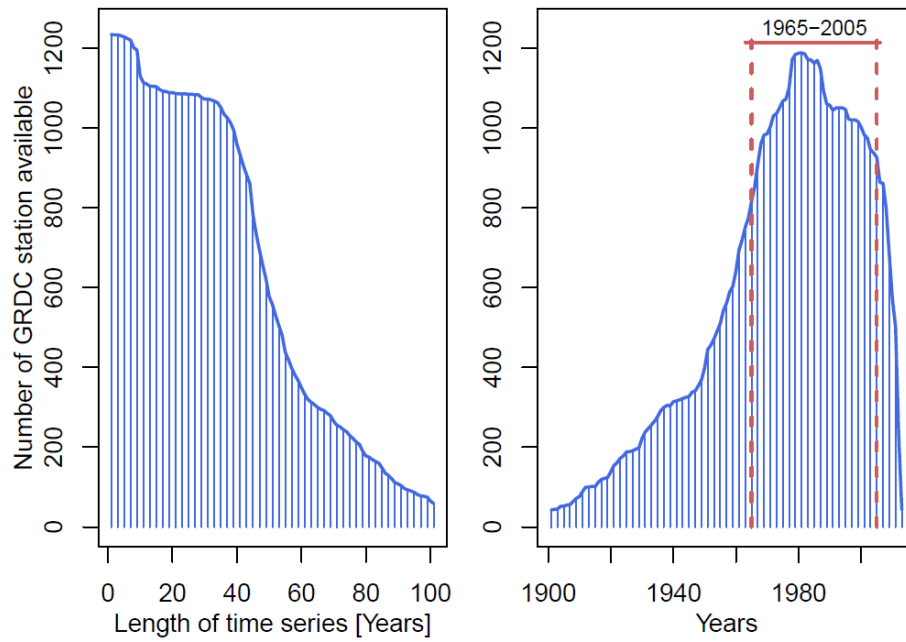


Figure 2. Length and time periods of daily discharge time series contained in the European Global Runoff Data Centre (GRDC) subset. Left panel shows the time series length. Right panel shows the number of stations, which have data available in that year for the period 1900-2010. Red lines indicate the time window 1965-2005 selected for the trend analysis.

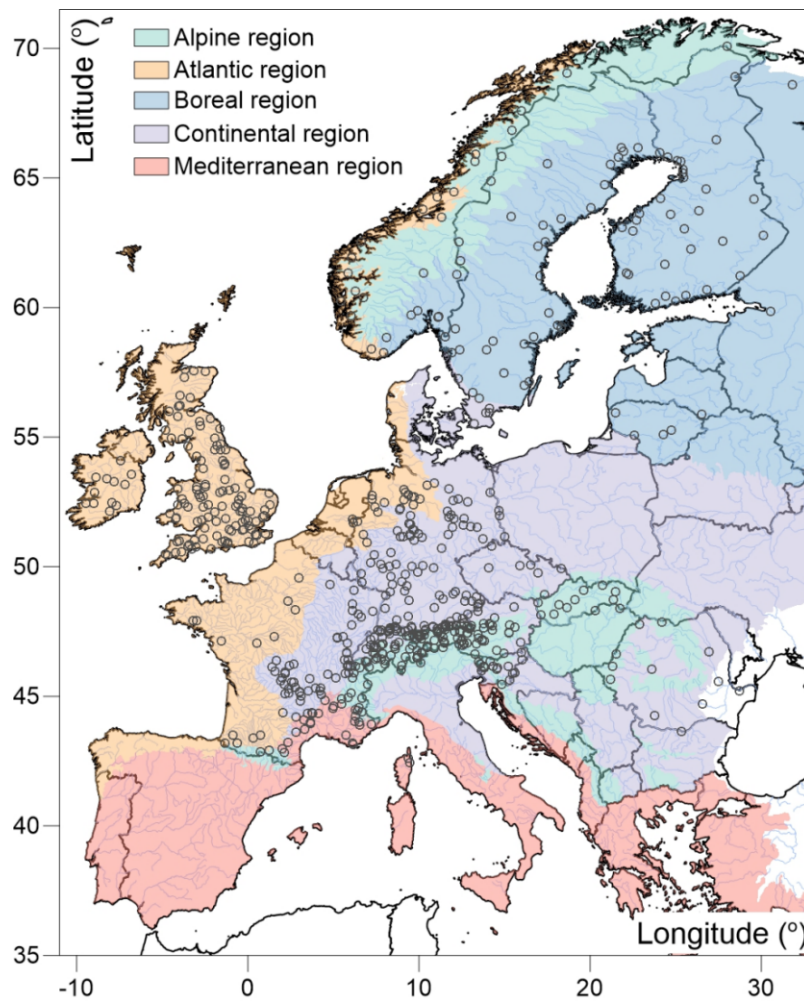


Figure 3: Five hydro-climatic regions in Europe based on a bio-geographical classification provided by the EEA. Points indicate the location of the 629 gauging stations.

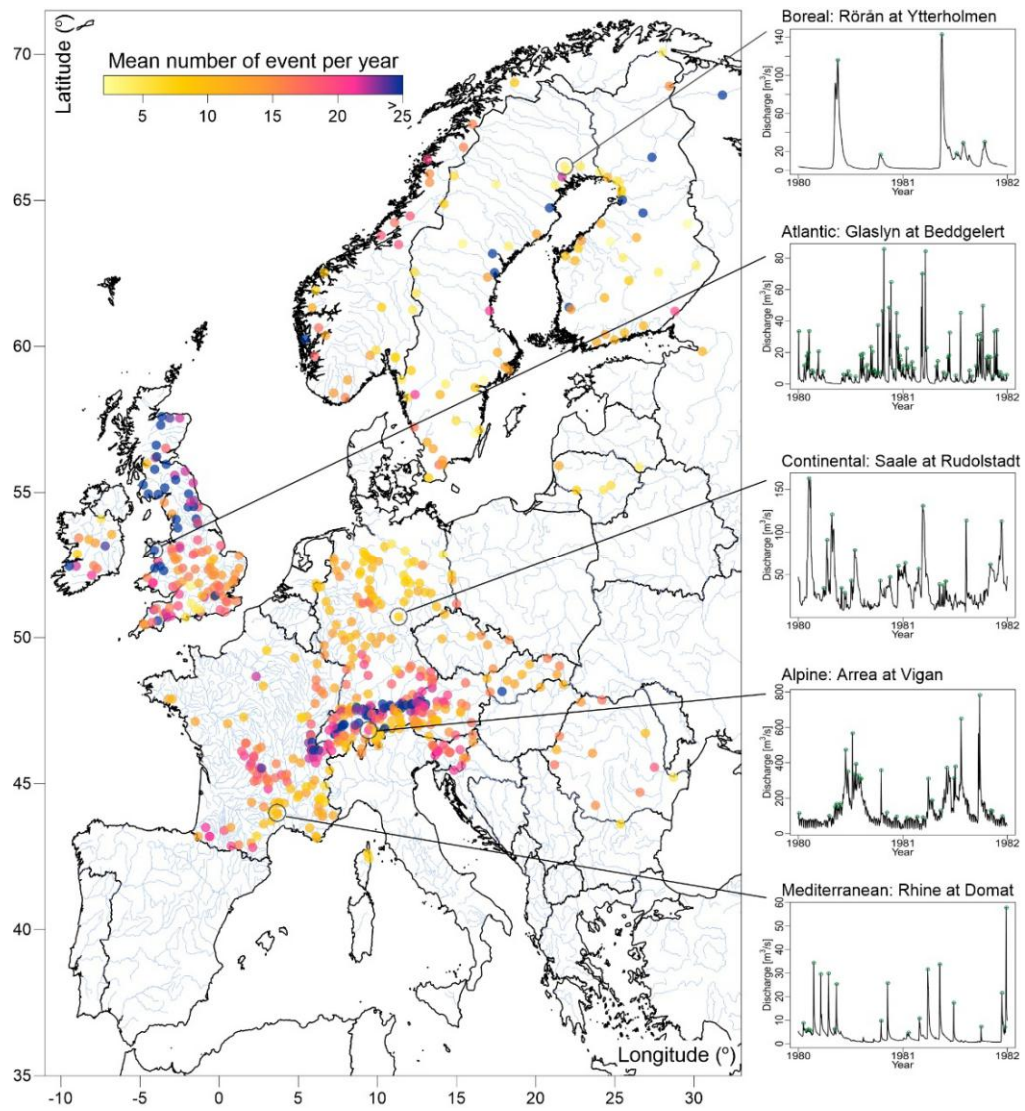


Figure 4. Mean number of independent discharge peaks per year at the selected 629 GRDC gauging stations. Panels on the right show examples of runoff hydrographs and discharge peaks for five sample gauging stations in the five hydro-climatic regions.

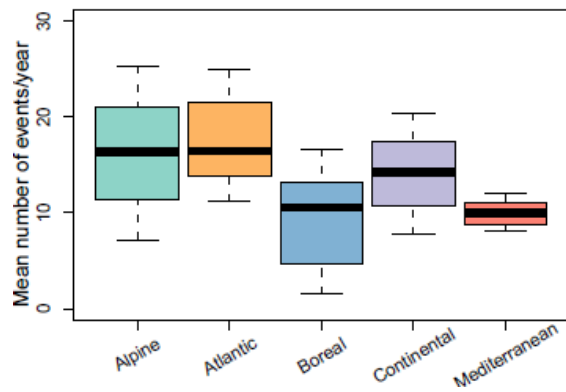


Figure 5. Mean number of independent discharge peaks per year identified by the baseflow-based algorithm, for each of the five hydro-climatic region. Bold line represents the 50% percentile, while boxes and whiskers show the 25%-, 75%-percentile, and the 10%-, 90%- percentiles, respectively.

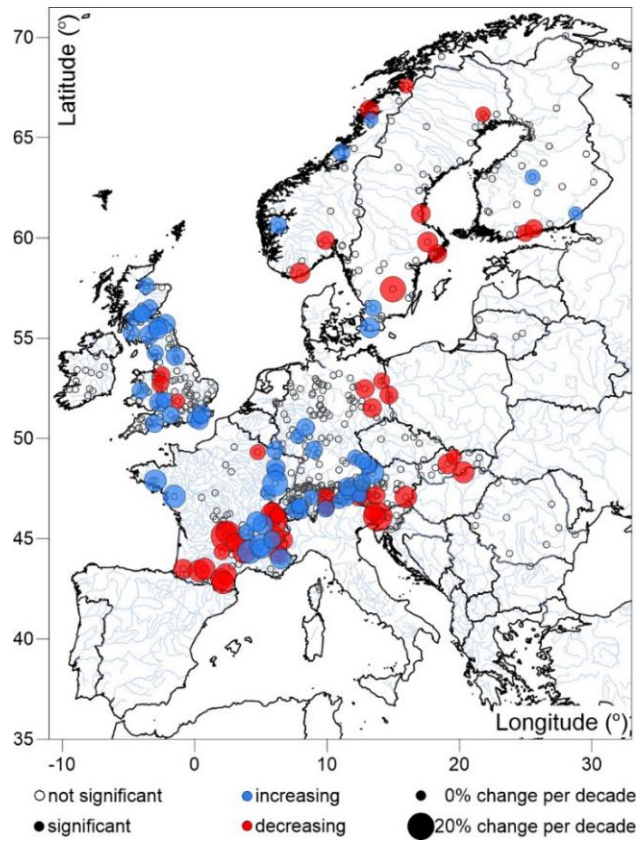


Figure 6. Trends in Annual Maximum Flood series (AMF) for the period 1965-2005. Filled symbols indicate statistical significant positive (blue) and negative (red) trends at 10% level of significance. Symbol size indicates the magnitude of change in the mean flood magnitude (% per decade).

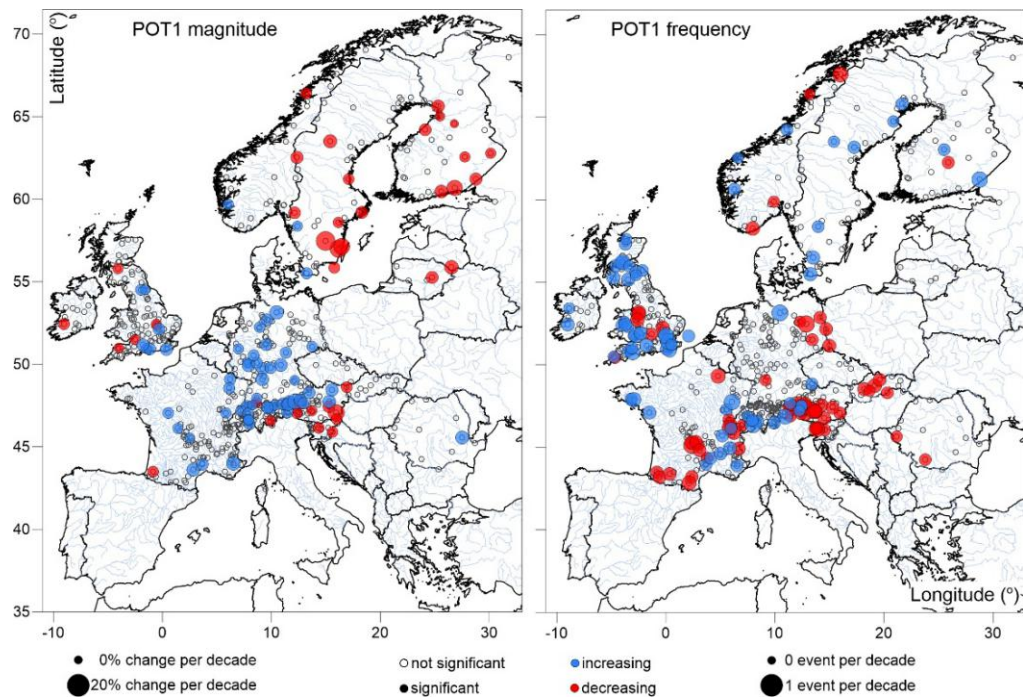


Figure 7. Trends in POT1 series. Left/right panel shows trends in flood magnitude/frequency. Filled symbols indicate statistical significant positive (blue) and negative (red) trends at 10% level of significance. Symbol size indicates the change in the mean flood magnitude (left), mean number of floods (right) exceeding the threshold in % per decade and in events per decade respectively.

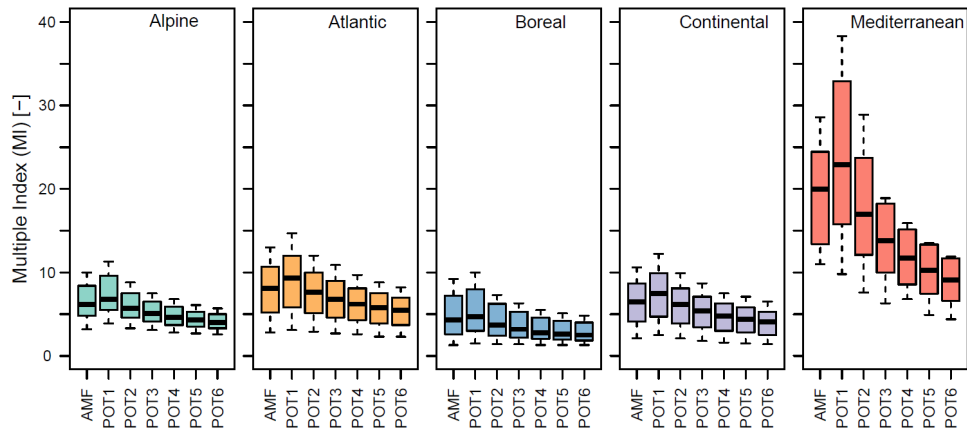


Figure 8. Multiple Index (MI) of the Annual Maximum Flood (AMF) and the different Peak Over Threshold (POT) flood series. For the latter thresholds of λ (mean number of peaks per year) are ranging from 1 (POT1) to 6 (POT6).

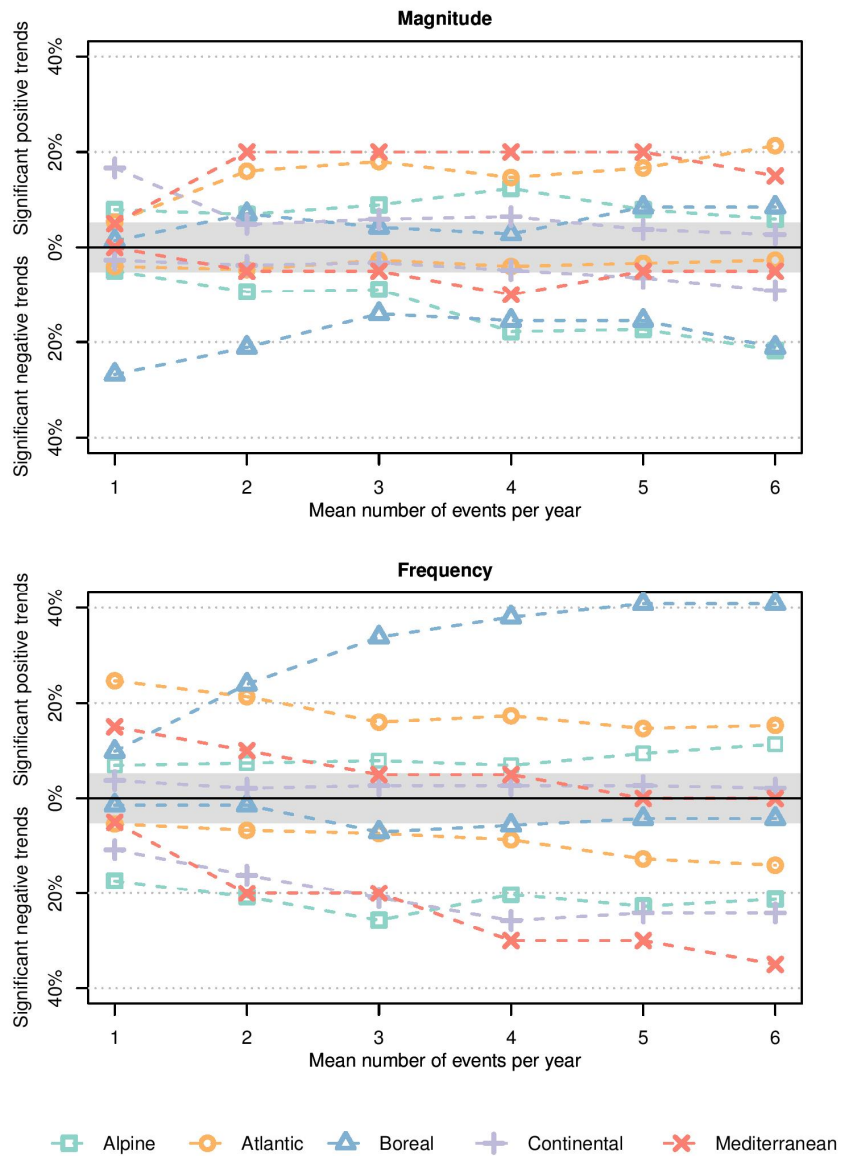


Figure 9. Percentage of stations exhibiting significant trends in magnitude and frequency at 10% level, with a threshold λ ranging from a mean of one to six events/year. Top and bottom panel show the sensitivity analysis in flood magnitude and frequency, respectively. Different colours and symbols indicate the 5 hydro-climatic regions. The grey band represents the percentage of station (5% in the positive semiaxis and 5% negative semiaxis) exhibiting trend that is expected to be detected by chance, given the significance level of the test.

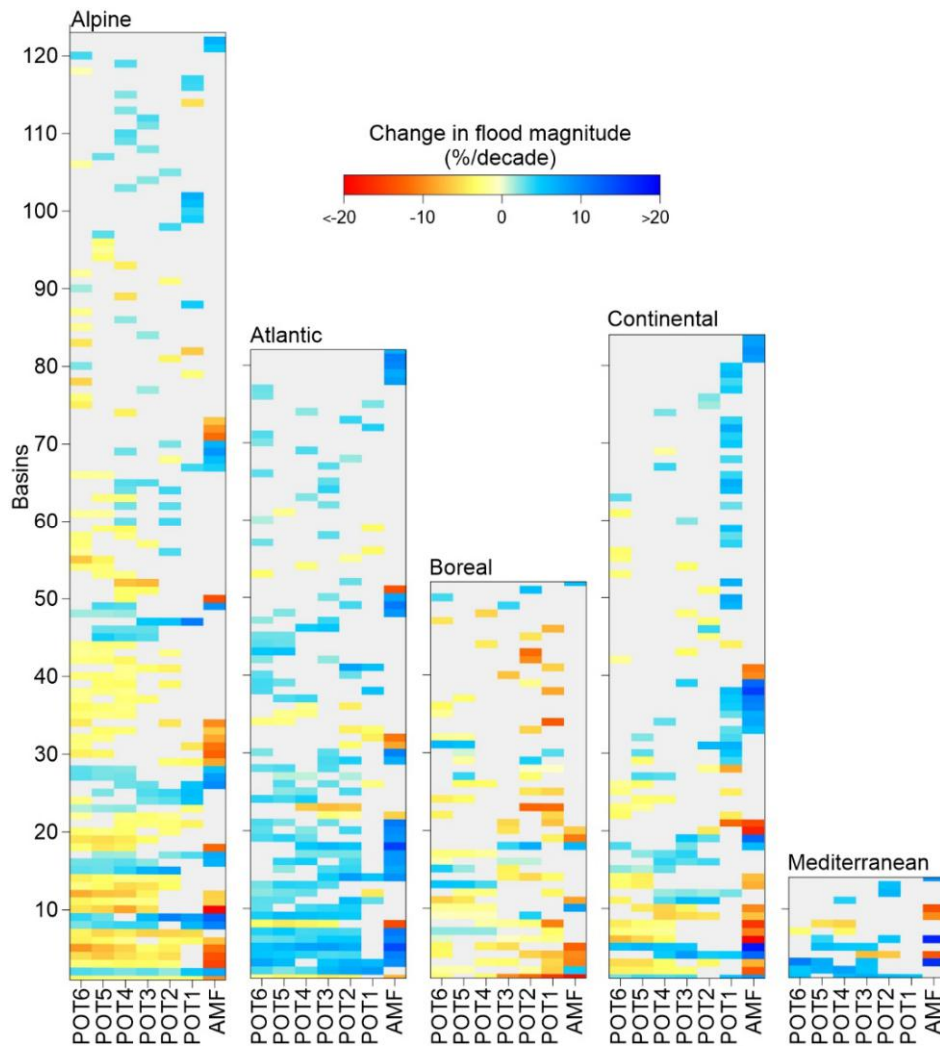


Figure 10. Summary of the significant trends detected at 10% level in the AMF

and the POT-M series. POT-M series are compiled for a mean number of exceedances λ ranging from 1 to 6. The colour scale indicates the intensity of the decadal change detected for significant trends, in % per decade, while grey colour is used when no significant trends are detected. Catchments are grouped into the five hydro-climatic regions of Europe and are sorted in a decreasing order (from the bottom) by the cumulative number significant trends detected in individual catchments over the different flood series.

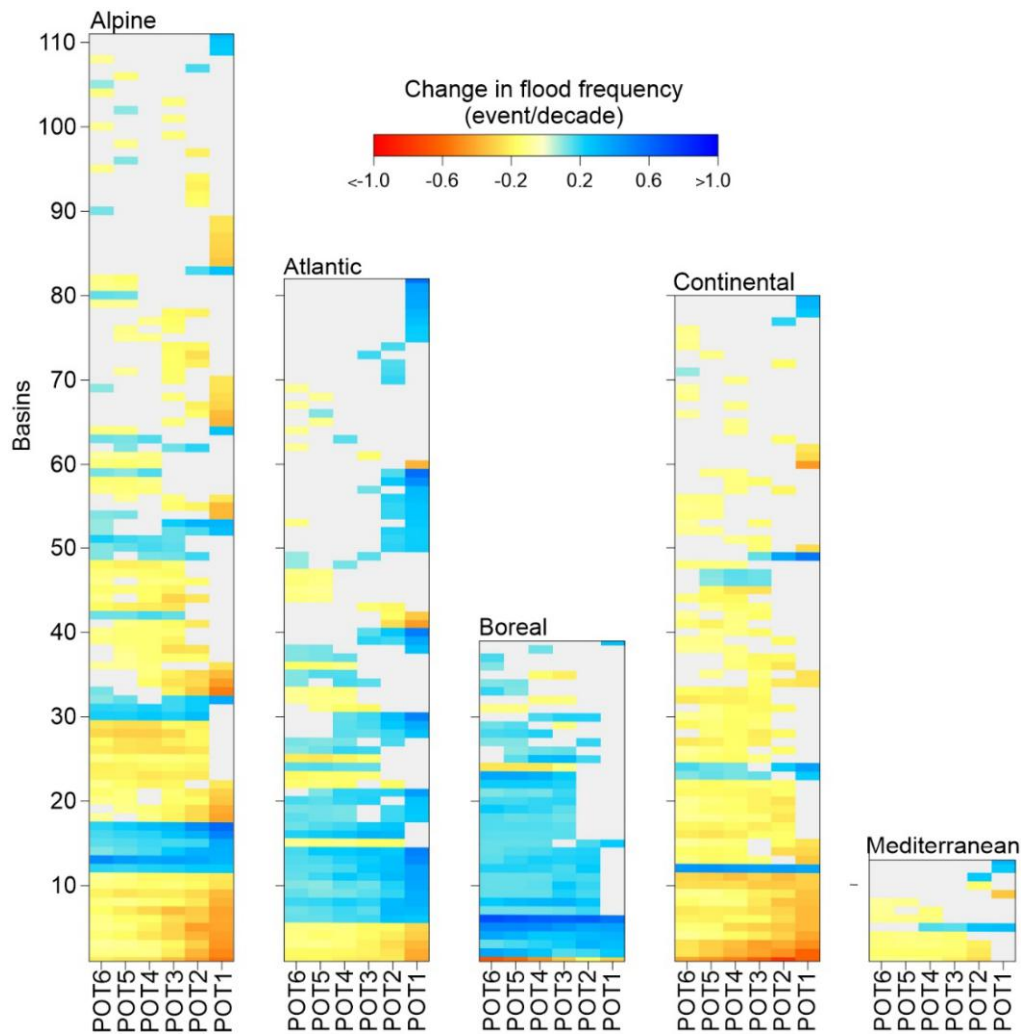


Figure 11. Summary of the significant trends detected at 10% level in the POT-F series. POT-F series are compiled for a mean number of exceedances λ ranging from 1 to 6. The colour scale indicates the intensity of the decadal change detected for significant trends, in % per decade, while grey colour is used when no significant trends are detected. Catchments are grouped into the five hydro-climatic regions of Europe and are sorted in a decreasing order (from the bottom) by the cumulative number significant trends detected in individual catchments over the different flood series.

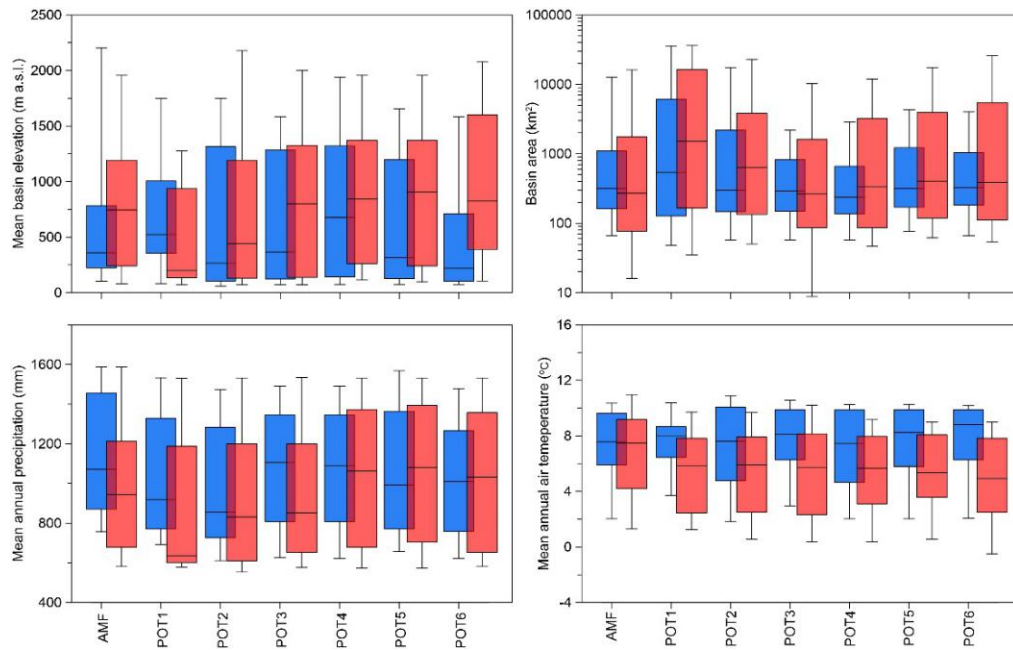


Figure 12. Distribution of selected physiographic characteristics of the

catchments exhibiting significant trends in flood magnitude at 10% level. Increasing or decreasing trends in flood magnitude are presented in blue or red colour, respectively.

Bold lines represent the 50%- percentile, while boxes and whiskers indicate the 10%-, 25%-, 75%- and 90%- percentiles.

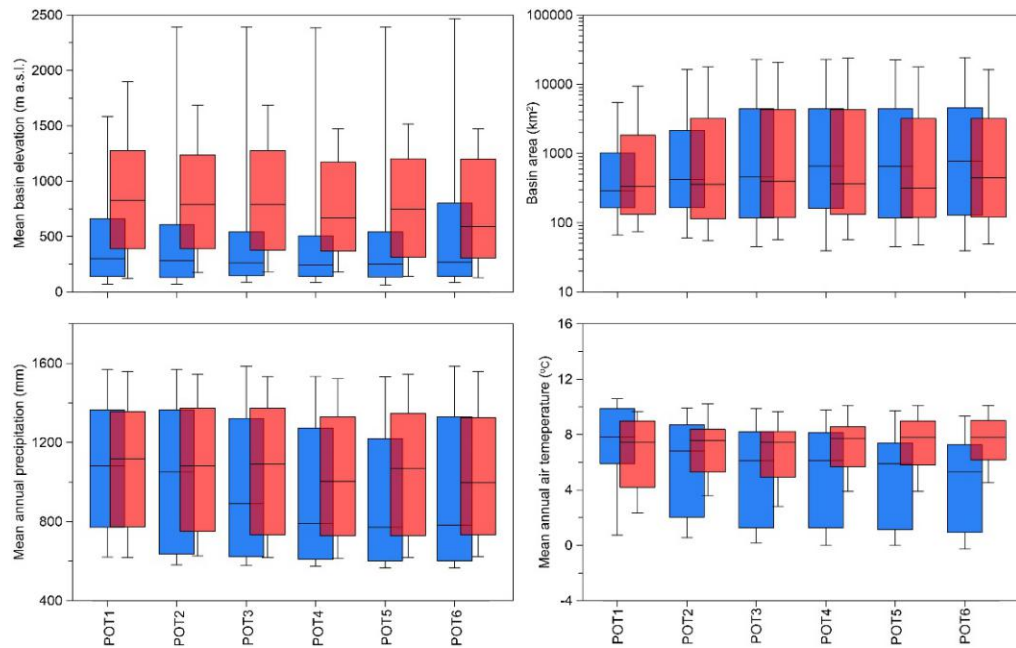


Figure 13. Distribution of selected physiographic characteristics of the catchments exhibiting significant trends in flood frequency at 10% level. Increasing or decreasing trends in flood magnitude are presented in blue or red colour, respectively. Bold lines represent the 50%- percentile, while boxes and whiskers indicate the 10%-, 25%-, 75%- and 90%- percentiles.

Table 1: Description of the five hydro-climatic regions (see also Fig. 3). The table contains the name of the regions, the main geographical position, number of stations located within, the CCM2 windows that cover the region and the predominant Köppen-Geiger climate classification.

Region	Geographical position	Number of stations	CCM2 windows	Predominant Köppen climate
Alpine	Central range systems	202	2000, 2002, 2003, 2005, 2007, 2008	Snow and polar
Atlantic	Northern islands/coasts	150	2000, 2001, 2003, 2008	Warm temperate - fully humid
Boreal	Northern Europe	71	2000, 2007, 2008, 2013	Snow - fully humid
Continental	Central Europe	186	2000, 2003, 2005, 2013	Warm temperate and snow - fully humid
Mediterranean	Southern Europe	20	2002, 2003	Warm temperate - summer dry

Table 2. Absolute number of stations exhibiting significant positive/negative trends at 10% level in flood magnitude detected in the POT-M series with a thresholds λ (a mean number of events per year) ranging from 1 (POT1-M) to 6 (POT6-M). The stations are grouped into the different hydro-climatic regions.

	Alpine	Atlantic	Boreal	Continental	Mediterranean
Number of stations	202	150	71	186	20
POT1-M	16/10	8/6	1/19	31/5	1/0
POT2-M	14/19	24/7	5/15	9/7	4/1
POT3-M	18/18	27/4	3/10	11/6	4/1
POT4-M	25/36	22/6	2/11	12/9	4/2
POT5-M	16/35	25/5	6/11	7/12	4/2
POT6-M	12/44	32/4	6/15	5/17	3/1

Table 3. Absolute number of stations exhibiting significant positive/negative trends at 10% level in flood frequency detected in the POT-F series with a thresholds λ (a mean number of events per year) ranging from 1 (POT1-F) to 6 (POT6-F). The stations are grouped into the different hydro-climatic regions.

	Alpine	Atlantic	Boreal	Continental	Mediterranean
Number of stations	202	150	71	186	20
POT1-F	14/35	37/8	7/1	7/20	3/1
POT2-F	15/42	32/10	17/1	4/30	2/4
POT3-F	16/52	24/11	24/5	5/39	1/4
POT4-F	14/41	26/13	27/4	5/48	1/6
POT5-F	19/46	22/19	29/3	5/45	0/6
POT6-F	23/43	23/21	29/3	4/45	0/7